JOURNAL OF GEOPHYSICAL RESEARCH, VOL. 103, NO. D24, PAGES 31,821–31,835, DECEMBER 27, 1998

An overview of GOES-8 diurnal fire and smoke results for SCAR–B and 1995 fire season in South America

Elaine M. Prins,[1] Joleen M. Feltz,[2] W. Paul Menzel,[1] and Darold E. Ward[3]

Abstract. The launch of the eighth Geostationary Operational Environmental Satellite (GOES-8) in 1994 introduced an improved capability for diurnal fire and smoke monitoring throughout the western hemisphere. In South America the GOES-8 automated biomass burning algorithm (ABBA) and the automated smoke/aerosol detection algorithm (ASADA) are being used to monitor biomass burning. This paper outlines GOES-8 ABBA and ASADA development activities and summarizes results for the Smoke, Clouds, and Radiation in Brazil (SCAR–B) experiment and the 1995 fire season. GOES-8 ABBA results document the diurnal, spatial, and seasonal variability in fire activity throughout South America. A validation exercise compares GOES-8 ABBA results with ground truth measurements for two SCAR–B prescribed burns. GOES-8 ASADA aerosol coverage and derived albedo results provide an overview of the extent of daily and seasonal smoke coverage and relative intensities. Day-to-day variability in smoke extent closely tracks fluctuations in fire activity.

1. Introduction

Biomass burning is a distinct biogeochemical process with links to the biosphere, atmosphere, and geosphere. The effects of biomass burning activities on the global environment are not well understood. In recent years the scientific research community has recognized the need to gain a better understanding of the extent of global biomass burning activities to assess the impact of these activities on surface and atmospheric processes and other biogeochemical interactions. Studies have suggested that biomass burning associated with deforestation and savanna management in the tropics is responsible for a significant portion of global trace gas emissions and aerosols [*Crutzen et al.*, 1985; *Andreae et al.*, 1988; *Crutzen and Andreae*, 1990; *Andreae*, 1991; *Levine*, 1991]. In the past, most discussions focused on the impact of biomass burning on net greenhouse warming from increased CO_2 and other trace gas emissions. Recent modeling and analysis efforts have addressed the direct and indirect radiative effects of biomass burning aerosols and the role they play in climate change calculations [*Twomey et al.*, 1984; *Penner et al.*, 1992, 1994; *Kaufman and Fraser*, 1997; *Christopher et al.*, 1996].

One of the largest areas of uncertainty lies in assessments of the total amount of biomass burned globally each year. The majority of biomass burning occurs in developing countries in the tropics and subtropics of Africa, South America, and Southeast Asia where remote sensing is often the best way to quantify the extent and distribution of fires and smoke coverage from the local to regional and continental scales. During the 1980s the utility of geostationary remote sensing to monitor active fires and aerosol transport was demonstrated in South America using the visible infrared spin scan radiometer atmospheric sounder (VAS) onboard the Geostationary Operational Environmental Satellites (GOES) [*Fishman et al.*, 1986; *Prins and Menzel*, 1992]. The GOES VAS automated biomass burning algorithm (ABBA) was developed at the Cooperative Institute for Meteorological Satellite Studies (CIMSS) to automatically detect and characterize active fires in this region [*Prins and Menzel*, 1994]. Although the GOES VAS ABBA provided new insight on the diurnal nature of fires and smoke transport, fire detectability and characterization was limited by the relatively coarse spatial resolution of the GOES VAS instrument. A new capability for geostationary diurnal monitoring of subpixel fire activity and aerosols was realized with the launch of GOES-8 in the spring of 1994. The GOES-8 offers higher spatial and temporal resolution, greater radiometric sensitivity, and improved navigation. The increased spatial resolution (4 km on GOES-8 versus 13.8 km on GOES-7) makes it possible to see much greater detail in the GOES-8 data, including land features and localized fire activity of the order of a few acres in size [*Menzel and Prins*, 1996a, b; *Prins and Menzel*, 1996a, b].

The 1995 fire season in South America was the first full fire season with operational GOES-8 coverage. The GOES VAS ABBA was adapted for GOES-8 application, and an initial version of the GOES-8 ABBA (version 1.0) was operational during the Smoke, Clouds, and Radiation in Brazil (SCAR–B, 1995) experiment. In support of the field program, CIMSS provided mission scientists with diurnal (3 hourly) information on the location, size, and mean temperature of subpixel fires as well as smoke transport throughout the Amazon Basin and the South Atlantic Ocean. GOES-8 satellite imagery, meteorological observations, model output from the U.S. National Center for Environmental Prediction (NCEP), and GOES-8 ABBA derived fire and smoke products were made available in near real-time via the University of Wisconsin Space Science and Engineering Center (UW-SSEC) SCAR–B web site [*Bywaters and Prins*, 1996]. The GOES-8 ABBA was subsequently modified on the basis of experience gained during the SCAR–B

[1]NOAA/NESDIS/ORA/ASPT, University of Wisconsin-Madison, Madison.
[2]Cooperative Institute for Meteorological Satellite Studies (CIMSS), University of Wisconsin-Madison, Madison.
[3]Intermountain Research Station, U.S. Forest Service, Missoula, Montana.

Paper number 98JD01720.
0148-0227/98/98JD-01720$09.00

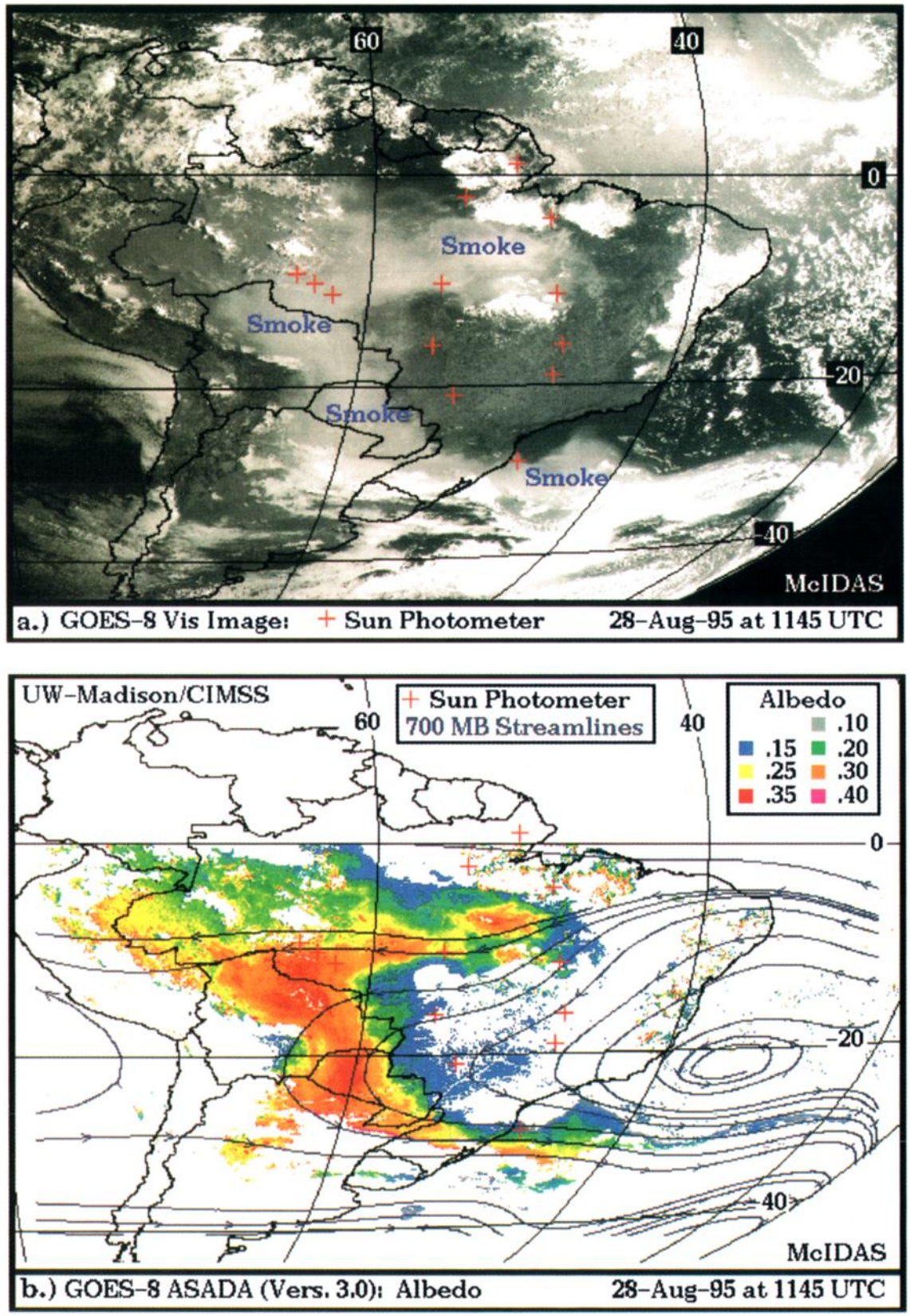

Plate 1. GOES-8 (a) visible and (b) ASADA-derived albedo product for August 28, 1995. Smoke is evident throughout the Amazon Basin, covering over 6 million km^2 and extending out over the Atlantic Ocean at the southern extent. The highest derived smoke albedos are 3 to 4 times greater than clear background values.

field program. The GOES automated smoke/aerosol detection algorithm (ASADA) was developed to document the extent and transport of biomass burning aerosols using GOES VAS [*Prins and Menzel*, 1996a, b]. A more robust algorithm was developed for GOES-8 applications using the Smoke, Clouds, and Radiation in California (SCAR–C, 1994) experiment and SCAR–B data sets. Diurnal GOES-8 data for June through October 1995 were reprocessed with version 5.5 of the GOES-8 ABBA. Daily summaries of aerosol coverage and relative loading were produced with the GOES-8 ASADA (version 3.0).

This paper presents a brief overview of changes made to the GOES-8 ABBA since the SCAR–B experiment and discusses recent GOES-8 ASADA development activities. A summary of the GOES-8 ABBA results for SCAR–B are presented and discussed in relation to the entire 1995 burning season. The GOES-8 ABBA results provide a unique survey of the type of vegetation burned and the spatial and temporal distribution of fires in Brazil and throughout South America. GOES-8 ASADA smoke coverage and derived albedo estimates are summarized for SCAR–B and the 1995 fire season. GOES-8 ASADA products catalogue the extent, transport, and relative intensity of biomass burning aerosols in South America and over the South Atlantic Ocean. GOES-8 ABBA fire size estimates are compared with ground truth values obtained for two prescribed burns during SCAR–B. This validation exercise offers some insight on the accuracy and reliability of GOES-8 ABBA fire size estimates.

2. GOES-8 ABBA Development Activities

The GOES VAS ABBA was developed at CIMSS to locate and provide estimates of subpixel fire size and temperature for a select region of South America (5°–15°S, 45°–70°W) and to determine trends in biomass burning in this region throughout the 1980s [*Prins and Menzel*, 1992, 1994]. The GOES ABBA is a dynamic multispectral thresholding algorithm which uses the shortwave infrared window (SIRW near 4 μm) and longwave infrared window (LIRW near 11 μm) bands to locate fire pixels. Similar fire identification algorithms have been developed and successfully implemented in global National Oceanic and Atmospheric Administration (NOAA) advanced very high resolution radiometer (AVHRR) applications [*Justice and Dowty*, 1994; *Flasse and Ceccato*, 1996]. The GOES ABBA is based on the sensitivity of the SIRW band to high-temperature subpixel anomalies and is an expanded version of a technique originally developed by Matson and Dozier for NOAA AVHRR [*Matson and Dozier*, 1981]. When the GOES ABBA locates a fire pixel, it incorporates ancillary data to correct for water vapor attenuation, surface emissivity and solar reflectivity, and subsequently uses numerical methods to solve for subpixel fire size and mean fire temperature [*Prins and Menzel*, 1994].

The latest version of the GOES-8 ABBA (version 5.5) includes a number of modifications to the initial version (version 1.0) which was operational for the SCAR–B field program. Version 5.5 takes advantage of the improved fire monitoring capabilities of the GOES-8 and also incorporates enhanced ancillary data sets. The GOES-8 imager oversamples the SIRW and LIRW instantaneous ground fields of view (IGFOV) along a scan line by a factor of 1.75. The impulse response is smeared over three samples. In order to take advantage of the oversampling, all possible fire pixels are identified and then reassessed to ensure that a single fire occurrence is not counted twice in adjacent pixels. The GOES-8 ABBA (version 5.5) also contains an adjustment to account for diffraction in the SIRW and LIRW. The GOES-8 instrument receives about 70% of the LIRW energy from one field of view (FOV) and 84% from 1.5 FOV; for the SIRW this becomes 85 and 92%, respectively. This suggests that the fraction of the pixel that is on fire is about 10% smaller for the LIRW band than for the SIRW band [*Menzel and Prins*, 1996a]. Incorporating a diffraction adjustment results in approximately a 10% decrease in fire size estimates. Finally, the GOES-8 navigation is maintained within 4 km at nadir by using over 100 landmarks in South America.

As a result of experience gained during SCAR–B, the GOES-8 ABBA (version 5.5) now includes several additional components to screen for subpixel and semitransparent cloud contamination and solar reflectance near local noon in the SIRW which often resulted in false positive fire identification in earlier versions. By incorporating an albedo test we have been able to screen out many of the subpixel cloud-contaminated pixels. The false positive fires associated with regional uniform semitransparent cloud contamination as well as solar reflectance near local noon were primarily due to ineffective background temperature determination techniques in version 1.0 of the GOES-8 ABBA. The techniques used in the earlier version resulted in a cold bias in background brightness temperature determination in these situations, which resulted in false positive fire identification. Although identification of semitransparent clouds continues to be difficult, version 5.5 of the GOES-8 ABBA now incorporates single and multiband thresholds as well as a SIRW minus LIRW histogram approach to screen for clouds and determine the background brightness temperatures. These changes have significantly reduced the occurrence of GOES-8 ABBA false positive fires. During the latter part of September and October it remains difficult to distinguish between fires and solar reflectance contamination near local noon in northeastern Brazil. Version 5.5 of the GOES-8 ABBA avoids areas with extreme solar reflectance contamination by screening out data where the solar zenith angle is less than 12.5° or when the computed reflected Sun angle is less than 12.5°. The scattering or reflected Sun angle (θ_r) is calculated from the following equation where θ_0 is the solar zenith angle, θ is the satellite zenith angle, and Ψ is the relative azimuth angle:

$$\cos \theta_r = \sin \theta \sin \theta_0 \cos \Psi + \cos \theta \cos \theta_0.$$

In previous versions of the GOES ABBA, bulk offsets of 2 and 4 K were added to the SIRW and LIRW brightness temperatures, respectively, to attempt to correct for the attenuation due to the nonopaque clouds that often form directly over fires in South America [*Prins and Menzel*, 1994]. The overall effect of including this correction was approximately a 75% overestimate in burned area calculations. Version 5.5 of the GOES-8 ABBA includes a variable offset for the SIRW and LIRW based on the difference between the fire pixel albedo and the background albedo. This variable offset was derived from a regression analysis of the difference between the observed and the background albedos and observed brightness temperatures for over 10,000 nonfire pixels. If the albedo for a given fire pixel is greater than 0.25 or if the difference between the observed albedo for the fire pixel and the background albedo is greater than 0.07, no offset for cloud attenuation is

Table 1. GOES-8 Multispectral Automated Smoke/Aerosol Detection Algorithm (ASADA)

Test	VIS Counts (0 ↔ 255)	Albedo (0 ↔ 1)	Solar Reflectance Angle, deg	SIRW Temp, K	LIRW Temp, K	DIRW Temp, K	SIRW–LIRW Temp, K	LIRW–DIRW Temp, K	Comment
1	20 ↔ 180								first pass to limit the brightness counts to values indicative of haze/cloud mix
2		0.15 ↔ 0.40 (land) 0.10 ↔ 0.40 (ocean)							solar zenith angle corrected albedo is used to further screen for clouds/surface reflectance over land and water
3			>20°						eliminates regions of high specular reflection and Sun glint
4				>285	>285		−4 ↔ +20		screens for opaque clouds, cirrus, and stratus
5					>285	>280		−4 ↔ +6	screens for low-level moisture, opaque clouds, and semitransparent cirrus
6	If a pixel has passed tests 1–5, check surrounding pixels and screen for cloud-edge pixels.								

attempted. The fire pixel is flagged as a fire but not processed for subpixel fire characteristics.

Another modification to the GOES-8 ABBA includes an expanded surface vegetation classification scheme [*Olson*, 1992] and associated 4 and 11 μm emissivity factors. Finally, NCEP model estimates of total precipitable water have been incorporated to account for water vapor attenuation in the 4 and 11 μm bands. The GOES-8 ABBA output includes fire location (latitude/longitude), estimates of fire size and temperature, 4 and 11 μm observed brightness temperatures, background brightness temperature and albedo statistics, ecosystem type, and a flag for nonprocessed fires to indicate the reason for not processing.

3. GOES-8 ASADA Development Activities

In South America and the South Atlantic multispectral GOES-8 data are also being used to identify smoke/aerosols associated with biomass burning and to distinguish smoke from multilevel clouds and low-level moisture using the GOES-8 automated smoke/aerosol detection algorithm (ASADA). The GOES-8 ASADA is based on an algorithm originally developed to identify smoke in GOES VAS imagery [*Prins and Menzel*, 1992; *Prins and Menzel*, 1996a, b]. Comparisons of GOES-7 and GOES-8 data collected during SCAR–C demonstrated the improved capability of the GOES-8 visible band for smoke plume detection [*Menzel and Prins*, 1996a]. The SCAR–C and SCAR–B data sets were used to test and improve the algorithm for GOES-8 applications.

The GOES-8 ASADA incorporates multispectral data including the visible (VIS, near 0.62 μm), SIRW, LIRW, and moisture sensitive longwave infrared window (often called the dirty window, DIRW near 12 μm) to map smoke/aerosols. The ASADA includes single and multiband difference thresholds, solar zenith angle corrected albedo calculations, and solar and satellite viewing geometry to distinguish smoke/haze from multilevel clouds, low-level moisture, and Sun glint. The algorithm is outlined in Table 1. The VIS is used to identify haze, the SIRW and LIRW screen out opaque, cirrus, and stratus clouds, and the DIRW indicates low-level moisture [*Prins and Menzel*, 1996a, b]. Sun glint often produces the same signature as smoke in visible imagery. In order to avoid those areas affected by Sun glint, regions with reflected Sun angles (θ_r) less than 20° are not processed. Furthermore, in South America the smoke/aerosols are most easily detected in the GOES-8 visible imagery near 1200 UTC which is coincident with a low solar zenith angle throughout much of the study area. By observing aerosols when the solar zenith angle is small, it is possible to avoid the effect of specular reflection over ocean and minimize the influence of variable surface reflectance over land. The revised algorithm also shows significant improvements in locating smoke in northwestern Brazil where it is often difficult to separate smoke from low-level moisture in the Amazon. Version 3.0 also includes a test to check for clouds in surrounding pixels. This test has significantly reduced false positive identification of smoke along gradients between clear and cloud-contaminated pixels.

The GOES-8 ASADA product consists of composite imagery and grids that provide a summary of the extent of smoke/aerosol coverage and smoke albedo estimates derived from the GOES-8 visible band (0.52–0.72 μm). This product gives a general indication of the smoke intensity. A GOES-8 visible image and the GOES-8 ASADA (version 3.0) derived albedo product for August 28, 1995, at 1145 UTC are shown in Plate 1. The GOES-8 ASADA is able to distinguish smoke from multilevel clouds seen in the GOES-8 visible image (Plate 1a) and track the smoke throughout the continent and out over the Atlantic Ocean ahead of a cold front. The smoke pall covers over 6 million km^2. GOES-8 ASADA derived smoke albedos are often 3 to 4 times higher than clear background values. A comparison of GOES-8 imagery with NCEP model output indicates that smoke transport over the Atlantic Ocean is at or above 700 mbar.

As with previous GOES instruments, the visible channels on GOES-8 were calibrated before launch, but there is no onboard calibration capability. In order to account for possible sensor gain changes after launch, postlaunch calibration is necessary. An initial study performed by the NOAA National Environmental Data Information Service (NESDIS) indicated that the visible sensor degraded by ~15% by August 1995 [M. Weinreb, personal communication, 1997]. This offset has been incorporated in the ASADA (version 3.0) albedo calculations. More quantitative analyses of aerosol optical depth will require additional GOES-8 visible calibration and validation efforts, including comparisons with the Sun photometer network in South America [*Holben*, 1996].

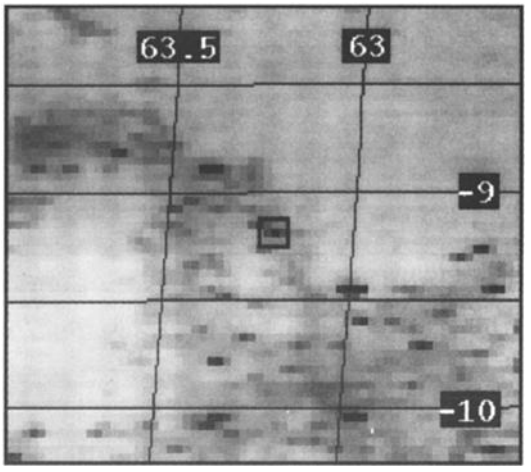

Figure 1. GOES-8 SIRW observation of the prescribed burn in Rondonia at 1815 UTC on September 4, 1995. The prescribed burn is outlined in black.

4. GOES-8 ABBA Results for SCAR–B Prescribed Burns

Validation of the GOES-8 ABBA was attempted with three prescribed burns initiated by the U.S. Forest Service during SCAR–B in Rondonia. A cattle pasture (~25 acres) was burned on September 2, 1995. There was widespread cloud cover on this day which prohibited GOES-8 analysis of this fire. The remaining two prescribed burns were slashed primary forest fires. On September 4, 1995, ~3.7 acres of forest in the state of Rondonia (9.2°S, 63.2°W) were ignited near 1300 LT (1700 UTC) [*Kauffman et al.*, 1997; D. Ward, personal communication, 1998; R. Babbitt, personal communication, 1998] and burned for several hours with smoldering evident for several days. The GOES-8 imagery displayed several fires in this region at that time making it difficult to isolate the prescribed burn. Ground truth reports indicated that the prescribed burn was the largest fire burning within a 5–8 km radius. GOES-8 analyses focused on the most intense fire pixel in the vicinity of the prescribed burn coordinates. A snapshot of the fire as observed in GOES-8 SIRW imagery at 1815 UTC is shown in Figure 1. The dark hot spots indicate fires throughout the region. The prescribed burn is outlined in black.

The fire was observed in the GOES-8 SIRW from 1745 UTC until ~2015 UTC. A faint signal was observed after this time. Table 2 provides a summary of the observed GOES-8 SIRW and LIRW observations and GOES-8 ABBA (version 5.5) estimates of subpixel fire size and temperature. The GOES-8 ABBA results at 1745 UTC indicated a fire size of ~8.9 acres burning at a temperature of 594 K. This estimate is nearly 2.5 times the actual fire size. This overestimate may be due to the large amount of biomass burned (over 355 Mg/ha of total above ground biomass (TAGB)) and intense flaming conditions within 1 hour after ignition [*Kauffman et al.*, 1997]. Fire size estimates at 1815, 1945, and 2015 UTC were similar to the ground truth estimates of fire size and temperature. At 1845 UTC the GOES-8 ABBA attempted to correct for cloud contamination as observed by the increase in albedo and decrease in the LIRW brightness temperature, but the correction was not sufficient, and the fire was not processed. At 1915 UTC the SIRW displayed the strongest fire signal. Although the fire was identified by the GOES-8 ABBA (version 5.5), the applied cloud correction was not sufficient in the LIRW band, and the fire pixel could not be processed.

A second slashed primary forest (~8.4 acres) plot within a few kilometers of the previous prescribed burn was ignited near local noon on September 6, 1995. Since no other fires were detected by GOES-8 in the near vicinity, identification of the fire was not a problem. Unfortunately, on this day there was significantly more cumulus cloud cover in Rondonia, limiting GOES-8 observations of the prescribed burn to three time periods. The fire was observed in the 1715, 1745, and 1815 UTC imagery. GOES-8 observations and fire size/temperature estimates are listed in Table 2. The largest fire signal was observed at 1715 UTC immediately after ignition. The elevated albedo (0.21) over the fire indicates substantial atmospheric attenuation. Although a cloud correction was applied, it was not sufficient, and the fire was not processed for subpixel size and temperature. At 1745 UTC the GOES-8 ABBA estimated the fire size at 2.0 acres burning at 744 K. By 1815 UTC the fire size estimate was 11.1 acres burning at a smoldering temperature of 506 K. This value is ~33% greater than the actual fire size. This prescribed burn was twice the size of the previous prescribed burn, yet the SIRW observed brightness temperatures were considerably lower due to cloud contamination. Subpixel fire size estimates are difficult to determine in these

Table 2. GOES-8 ABBA Results for Two Prescribed Burns During SCAR–B

	GOES-8 Observations			GOES-8 ABBA Fire Estimates	
Time, UTC	SIRW Temperature (K) Observed, Background	LIRW Temperature (K) Observed, Background	Albedo Observed, Background	Area (Acres)	Temperature, K
		Prescribed Burn: September 4, 1995			
1745	320.6, 305.8	302.1, 300.8	0.16, 0.15	8.9	594
1815	326.4, 305.6	301.8, 301.1	0.15, 0.15	2.2	838
1845	326.4, 304.9	297.8, 300.3	0.18, 0.16	INP	INP
1915	328.9, 304.3	299.4, 299.8	0.18, 0.17	INP	INP
1945	320.0, 303.4	299.1, 299.0	0.20, 0.17	4.2	686
2015	314.2, 302.1	298.9, 298.3	0.19, 0.18	2.8	678
		Prescribed Burn: September 6, 1995			
1715	318.9, 305.6	298.1, 297.9	0.21, 0.14	INP	INP
1745	317.1, 304.8	296.4, 297.2	0.19, 0.14	2.0	744
1815	311.6, 304.2	298.7, 297.7	0.13, 0.13	11.1	506

INP indicates the fire was identified but not processed.

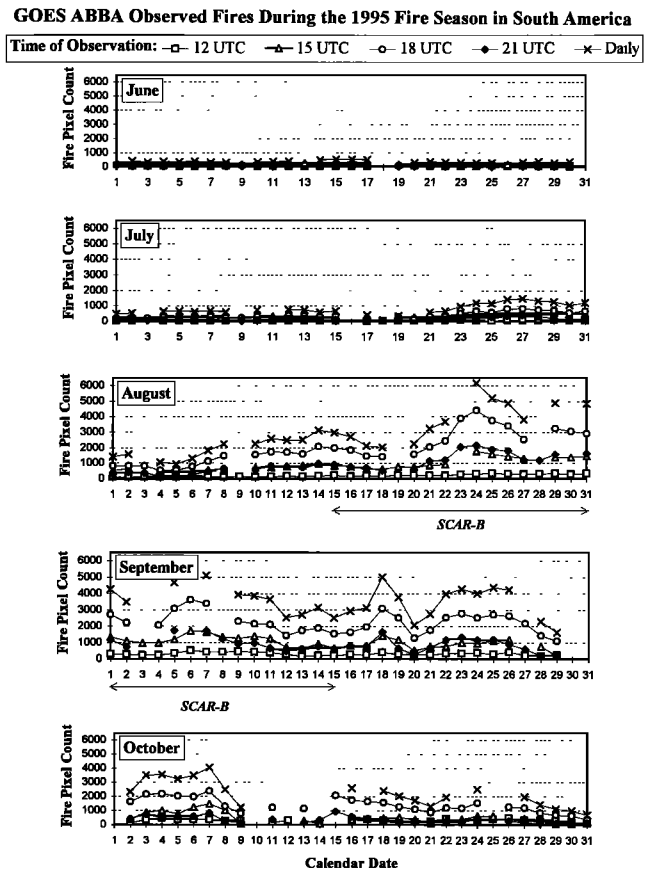

Figure 2. GOES-8 ABBA diurnal fire pixel counts for the 1995 fire season at 1145, 1445, 1745, and 2045 UTC. The figure also shows a plot of all unique fire pixel counts on days when all four time periods were available.

cases. The greatest source of error in the GOES-8 fire size estimates can be attributed to inaccurate corrections for atmospheric attenuation and subpixel semitransparent clouds [*Prins and Menzel*, 1992].

Although limited in scope, these validation examples suggest that the GOES-8 ABBA can identify fires that are of the order of a few acres in size and that fire size and temperature estimates are typically in line with ground truth observations. Comparisons with ground truth observations made in Brazil during SCAR–B and in the state of Washington during SCAR–C (California) indicate that at times the GOES-8 ABBA overestimates fire size by 20 to 50% [*Prins and Menzel*, 1996b]. It is also important to note that the GOES-8 ABBA fire size and temperature estimates only provide an instantaneous assessment of the average fire characteristics at the observation time and cannot distinguish the complex behavior associated with subpixel fire activity. Although the GOES-8 ABBA overestimated the fire size at one time period for both of the SCAR–B prescribed burns, these examples show the utility of considering a time series of half hourly GOES-8 ABBA results for a given fire to get a more accurate appraisal of subpixel fire characteristics. By analyzing a time series of observed 4 and 11 μm brightness temperatures and GOES-8 ABBA fire size estimates, it is possible to screen out the outliers and focus on the strongest cloud-free signals and trends in the progression of the fire.

5. Diurnal GOES-8 ABBA Results for SCAR–B and 1995 Fire Season in South America

5.1. The 1995 Fire Season

Multispectral GOES-8 data were collected every 3 hours from June to October during the 1995 fire season in South America. The study region extended from 0° to 40°S and from 35° to 75°W, including major biomass burning centers in Brazil, Peru, Bolivia, Paraguay, Uruguay, northern Argentina, and Chile. Data collected at peak burning times (1145, 1445, 1745, and 2045 UTC) were processed with version 5.5 of the GOES-8 ABBA. A time series showing GOES-8 ABBA 3 hourly and daily unique fire pixel counts is presented in Figure 2. The fire pixel counts include GOES-8 ABBA processed fire pixels, nonprocessed saturated fire pixels, and nonprocessed cloud-contaminated fire pixels. The daily unique fire pixel counts were determined by considering all fire pixels detected throughout the day. Fire pixels located within 5 km of each other at different time periods were considered to represent the same unique fire. For multiple detections of the same fire occurrence consisting of processed and nonprocessed cloudy or saturated fire pixel samples, the processed fire pixel with the greatest SIRW brightness temperature signature was chosen to represent this fire. If none of the samples were processed, the sample with the greatest SIRW signature was chosen. Figure 2

Table 3. Overview of GOES-8 ABBA Results for SCAR–B and 1995 Fire Season in South America

	Time, UTC				Total Fire Pixels	Total Unique Fire Pixels
	1145	1445	1745	2045		
			1995 Fire Season			
Processed fire pixels	23,747	75,572	135,376	61,176	295,871	244,250
Processed fire pixel burned area, km^2	2,143	14,069	17,261	2,939	36,412	31,124
Nonprocessed saturated fire pixels	111	1,510	5,684	425	7,730	4,013
Nonprocessed cloud covered fire pixels	2,118	4,018	26,012	2,941	35,089	25,903
Total fire pixels	25,976	81,100	167,072	64,542	338,690	274,166
Estimated total fire pixel burned area, km^2	2,344	15,098	21,302	3,101	41,845	34,936
			SCAR–B			
Processed fire pixels	8,743	31,100	57,388	29,816	127,047	99,982
Processed fire pixel burned area, km^2	792	5,690	6,678	1,366	14,526	11,837
Nonprocessed saturated fire pixels	19	910	2,957	180	4,066	1,915
Nonprocessed cloud covered fire pixels	657	1,732	10,000	1,278	13,667	9,442
Total fire pixels	9,419	33,742	70,345	31,274	144,780	111,375
Estimated total fire pixel burned area, km^2	853	6,173	8,186	1,433	16,645	13,182

only includes a plot of daily unique fire pixel counts on days where all four time periods were available.

The majority of the fires were observed during the months of August and September. There was also a considerable amount of fire activity during the first week of October. The greatest number of fires were detected during the final two weeks of August with a maximum on August 24, 1995. On this day, ~4400 fire pixels were detected at 1745 UTC with a daily total of over 6000 unique fire pixels. Throughout the season the diurnal signature is clearly evident with peak burning occurring in the early to midafternoon local time (1745 UTC). The number of fire pixels observed at this time is typically 2 to 3 times greater than that observed 3 hours earlier or later and nearly 7 times greater than at 1145 UTC. An analysis of the diurnal fire results indicates that although most fire pixels were detected in the early afternoon, many of the fire pixels observed at the other time periods represent unique occurrences not detected at 1745 UTC. The daily total of unique fire pixels is typically 65% greater than the value at 1745 UTC. This is important to consider when using polar orbiting satellites to monitor fire activity. The NOAA 14 afternoon overpass provides the only AVHRR observation of fire activity during peak burning times and cannot characterize the diurnal fire activity.

A composite of all fire pixels detected with the GOES-8 ABBA during the 1995 fire season is shown in Plate 2. The red markers indicate fire pixels that were processed with the GOES-8 ABBA for subpixel fire size and temperature. The yellow markers depict saturated fire pixels, and blue represents fire pixels which could not be processed due to significant cloud cover. The majority of the fire activity was concentrated along the perimeter of the Amazon in the Brazilian states of Maranhao, Tocantins, Para, Mato Grosso, Amazonas, Rondonia, and Acre. There was also considerable activity in Bolivia, Paraguay, and northern Argentina. Although fires were generally evident throughout the study area at all time periods the amount of fire activity varied greatly. There were also noticeable differences in the spatial distribution of fire pixels. The 1745 and 2045 UTC composites show more fire activity in Para and Amazonia and in the far western portion of the study area. The 1745 UTC composite clearly shows distinct burning patterns along rivers and in areas with recent road construction and associated settlements within the Amazon Basin. The spatial distribution of fires depicted in this figure shows patterns and details similar to those identified by *Skole and Tucker* [1993] in their analysis of deforestation observed in Landsat data in 1988.

Table 3 provides an overview of the total number of GOES-8 ABBA detected fire pixels and area burned during SCAR–B and the 1995 fire season. Throughout the season at all time periods, only 2.5% of the detected fire pixels were not processed due to saturation, and 10% of the fire pixels were not processed due to cloud contamination. To get an estimate of area burned by the nonprocessed saturated and cloudy fire pixels, an average fire pixel size was determined from the processed fire pixels and used to estimate the total area burned by the saturated and cloudy fire pixels. This extrapolation probably underestimates the fire size for saturated fire pixels but provides a minimum estimate of fire size for these cases. An estimate of the total area burned in processed, saturated, and cloud-contaminated fire pixels is listed in Table 3 for each time period. At 1745 UTC, over 167,000 fires were detected; ~81% were processed with the GOES-8 ABBA burning over 17,200 km^2. By including estimates for saturated and cloudy fire pixels this value increases to over 21,300 km^2. Similar statistics are presented for 1145, 1445, and 2045 UTC. A summary of all fire pixels detected by the GOES-8 ABBA throughout the day for the entire season is presented in column 6 of Table 3 which shows that during June through October 1995 over 338,690 fire pixels were detected with the GOES-8 ABBA with an estimated total burned area of 41,845 km^2. These estimates decrease by less than 20% when only unique fire pixel occurrences are considered (see column 7 of Table 3). To obtain a reliable estimate of fire activity, these results show that it is necessary to monitor fires throughout the day, not only at peak burning times.

Plate 3 summarizes the distribution of burning by ecosystem type. During the 1995 fire season, over 90% of the detected fire pixels occurred in six ecosystem types, although the majority of the fires were located in ecosystems 29 (seasonal tropical broadleaf, 35%), 43 (savanna/grassland/seasonal woods, 27%), 41 (mild/warm/hot grass/shrub, 19%), and 59 (succulent and thorn woods or scrub, 6%). At 1145 and 1445 UTC, ~30% of the fires occurred in ecosystem 29. This increased to nearly 40% at 1745 and 2045 UTC. Approximately 34% of the fires at 1145 UTC occurred in ecosystem 41. The burning in this ecosystem decreased to 24% at 1445 UTC and continued to decrease to 17% at 1745 UTC and 13% at 2045 UTC. Burning in ecosystem 43 increased from 14% at 1145 UTC to 27% at 1445 UTC and 1745 UTC and was a maximum of 31% at 2045 UTC. Over 6% of the fires at 1145 UTC occurred in ecosystem 31 (mild/hot farmland and settlements). Little activity was observed in this ecosystem later in the day. These distributions indicate that while fires in the grass/shrub and farmland/settlement ecosystems tend to occur more during the morning, burning in the seasonal tropical broadleaf and savanna/seasonal woods occurs predominantly during the afternoon. A comparison between primary ecosystem types revealed only small differences (less than 10%) in fire size and temperature estimates.

5.2. SCAR–B

The SCAR–B field program coincided with the height of the burning season in August and September 1995 as shown in Figure 2. A summary of the GOES-8 ABBA (version 5.5) results for SCAR–B is outlined in Table 3. The number of fires detected by the GOES-8 ABBA for SCAR–B reflects ~40% of the total burning for the 1995 fire season. The diurnal signature and ecosystem distribution in burning during SCAR–B was similar to what was observed during the rest of the season. The distribution of fire pixels and burned area for SCAR–B in comparison with the 1995 fire season is presented in Plate 4. Plates 4a and 4b show the distribution of fires (on a 0.25 km grid) at 1745 UTC for June through October 1995 and SCAR–B, respectively. The distribution patterns are quite similar, although burning in Bolivia appears to be more pronounced in the seasonal composite. In both cases the majority of the fires were located along the boundary between the seasonal tropical forests and the savanna/grasslands with relative maximums in the states of Maranhao, Tocantins, Mato Grosso, Rondonia, Acre, and south central Bolivia. This distribution was also observed in NOAA AVHRR imagery (S. Christopher, personal communication, 1998). Both the seasonal and the SCAR–B fire pixel count composites show burning along the major rivers and roads in Para and Amazonas. The burned area composites (Plates 4c and 4d) generally display many of the same features and reflect the distribution seen in the fire pixel count composites. The largest burned areas were located in regions which were previously deforested

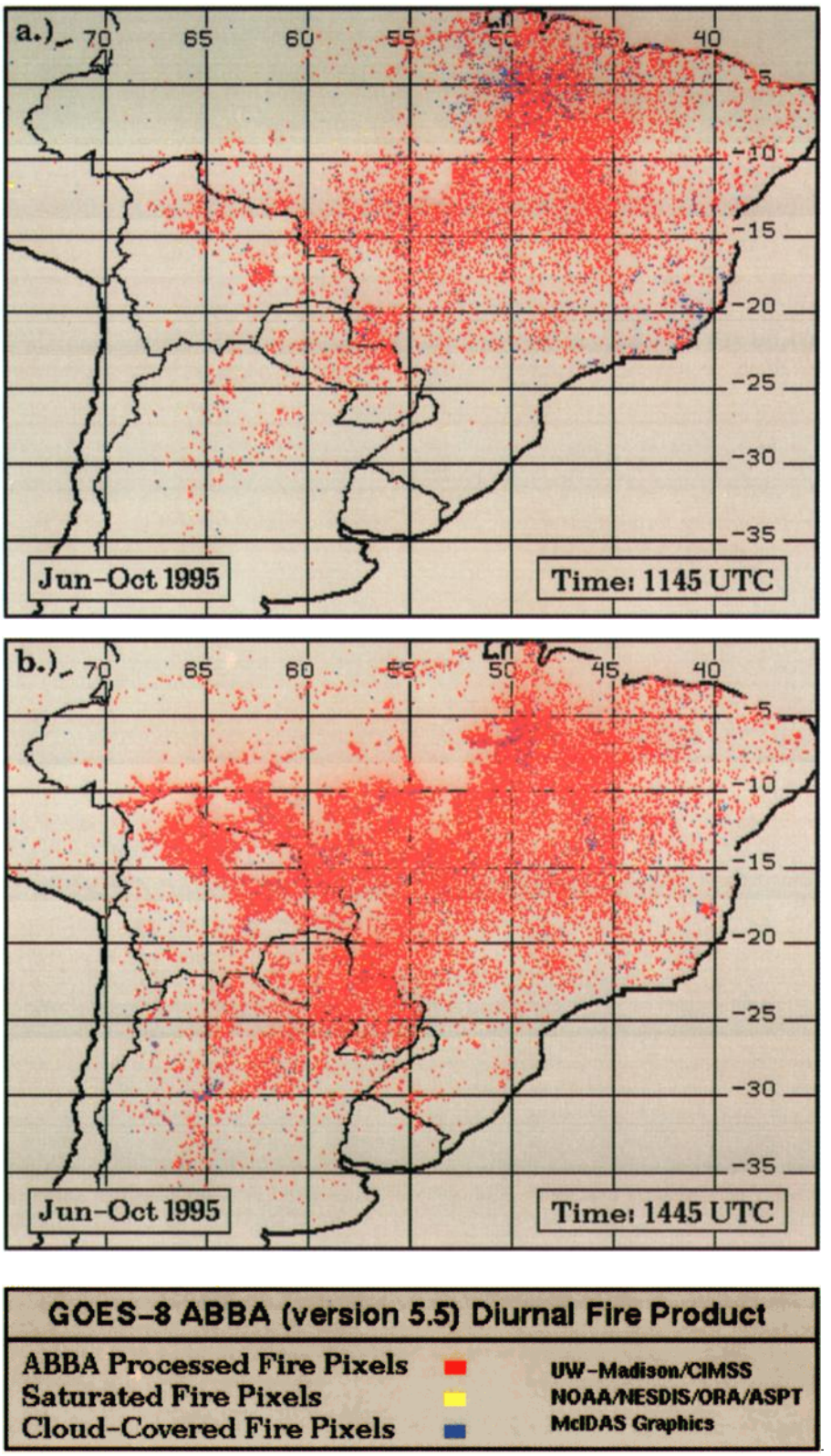

Plate 2. This composite shows the locations of all GOES-8 ABBA (version 5.5) detected fire pixels at (a) 1145 UTC, (b) 1445 UTC, (c) 1745 UTC, and (d) 2045 UTC during the 1995 fire season (June–October 1995). Red markers represent GOES-8 ABBA fire pixels that were processed for subpixel size and temperature estimates; yellow indicates nonprocessed saturated fire pixels; blue depicts fire pixels which could not be processed due to cloud cover.

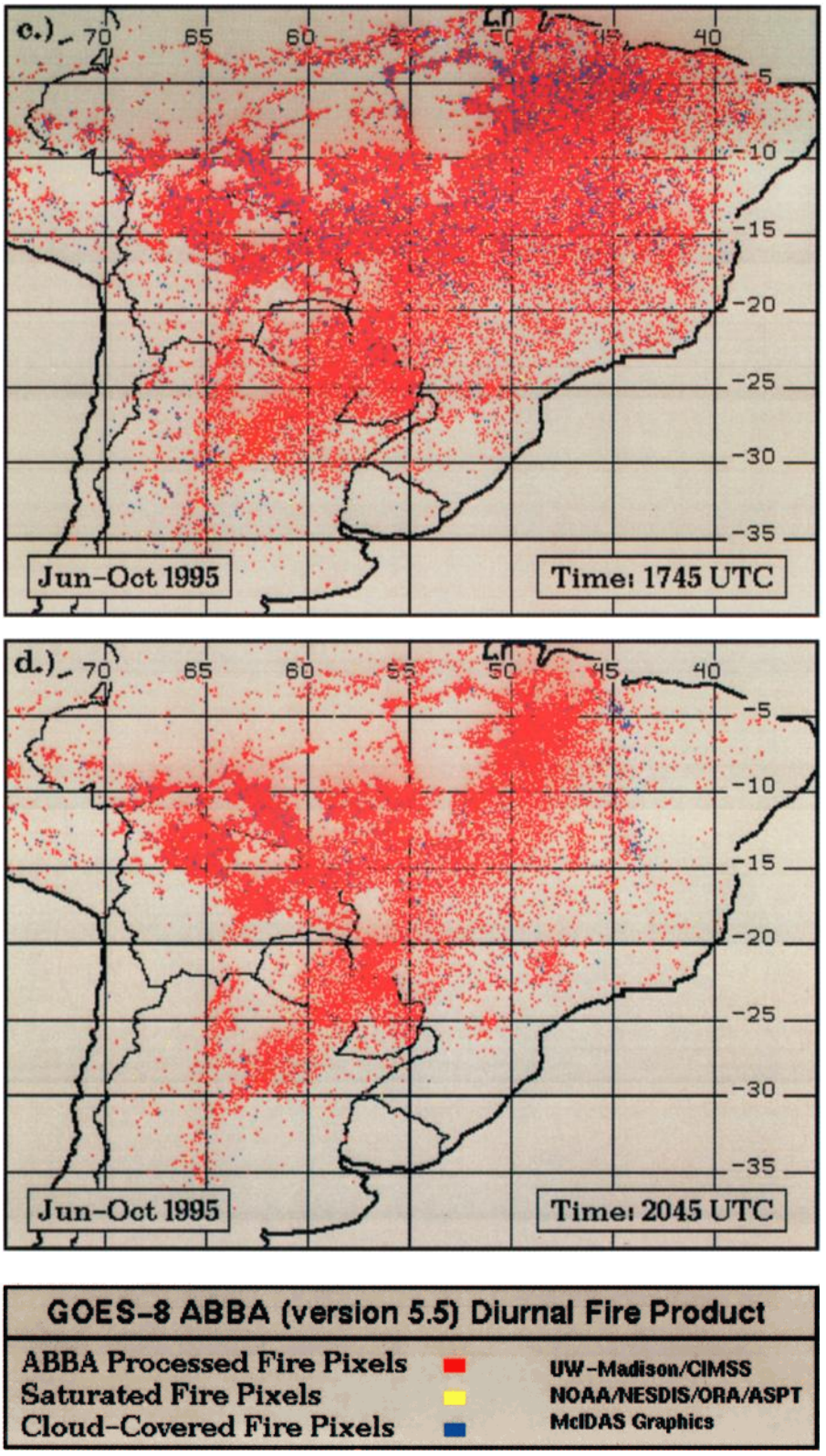

Plate 2. continued

along the interface between the primary forest and the cerrado. In both the SCAR–B and the seasonal fire pixel count composites (Plates 4a, 4b) some of the highest fire pixel counts are located in Rondonia, yet the burned area estimate composites (Plates 4c, 4d) do not reflect this intensity and may indicate that the fires are smaller in this region. In southeastern Brazil the composites show some fire activity, but they probably do not reflect the actual amounts. Many of the fires in this area are grassland fires which burn very quickly and do not have a strong thermal signature.

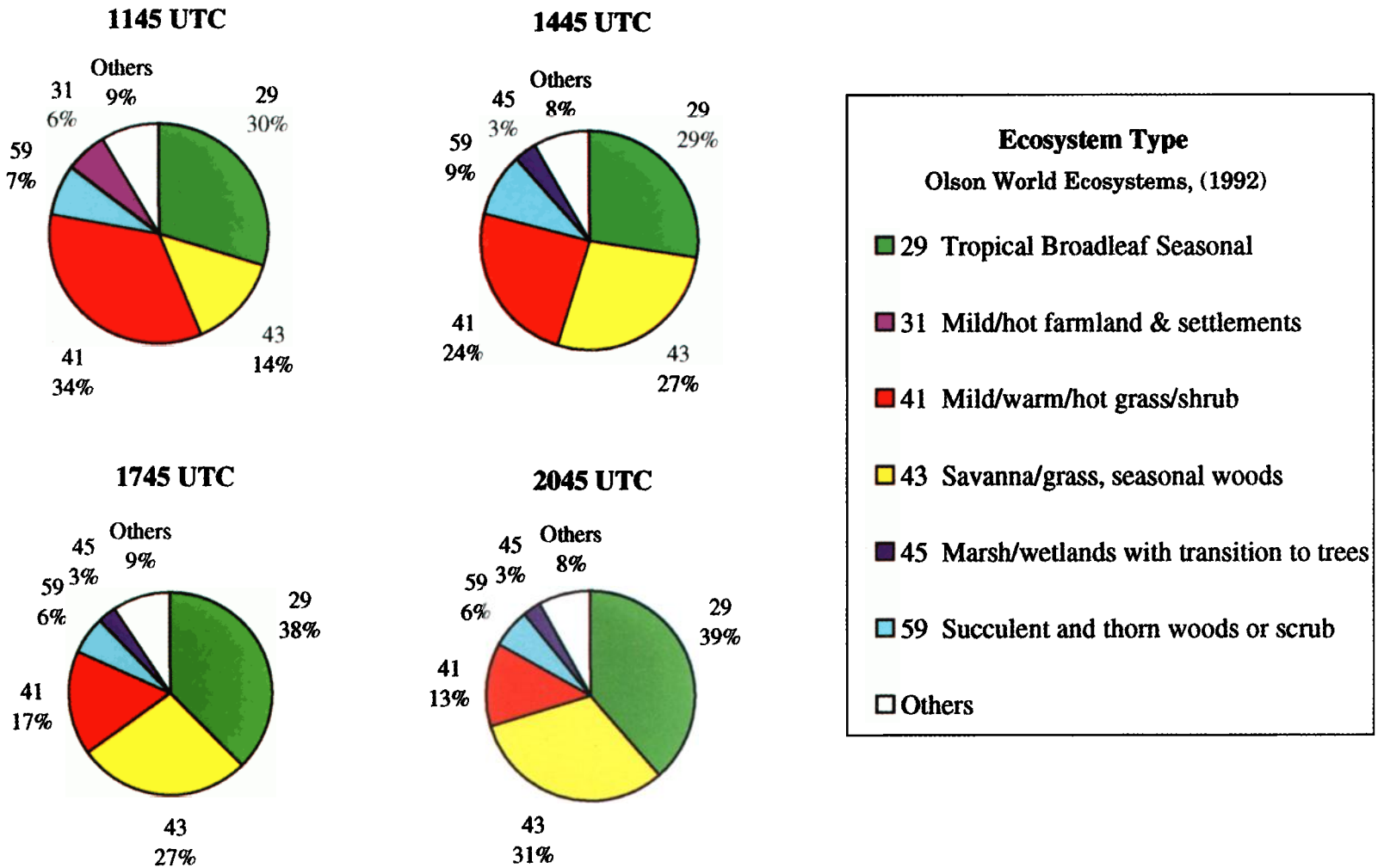

Plate 3. Diurnal distribution of burning by ecosystem type [*Olson*, 1992] during the 1995 fire season as determined by the GOES-8 ABBA.

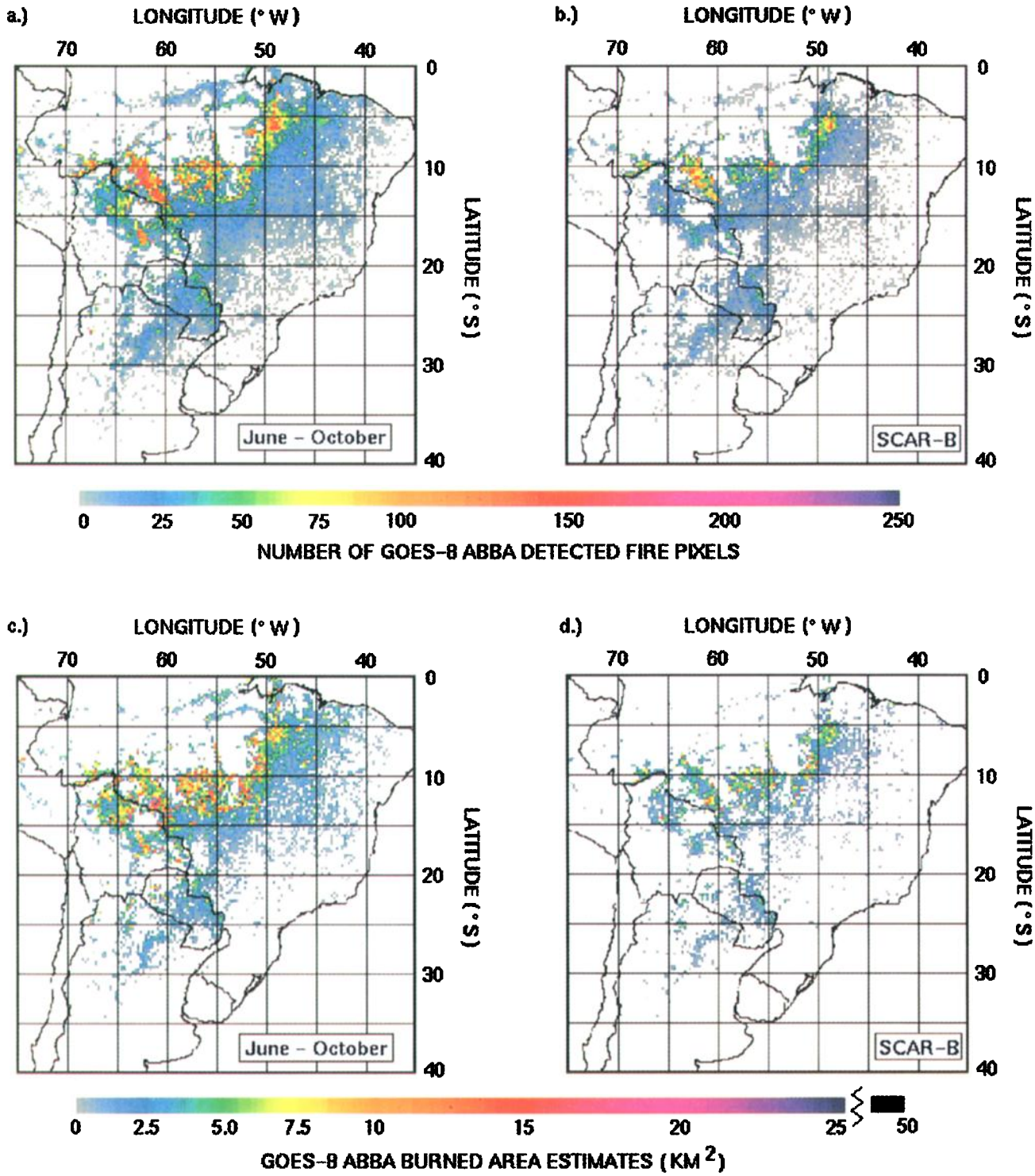

Plate 4. These composites show the distribution of GOES-8 ABBA fire pixel counts and burned area estimates at 1745 UTC for SCAR–B (Plates 4b, 4d) and the 1995 fire season (Plates 4a, 4c) on a 0.25° grid.

The number of GOES-8 ABBA (version 5.5) detected saturated and processed fire pixels and fire size estimates are significantly different from the values reported during SCAR–B with version 1.0. Overall version 5.5 results show less than a 10% decrease in fire pixel counts at 1445 and 1745 UTC and large increases at 1145 UTC (300%) and 2045 UTC (180%). On days with significant subpixel cloud contamination at 1445 and 1745 UTC the number of fire pixels reported with version 5.5 is 66% less. Subpixel cloud contamination was primarily an issue during the second week of September. Fire size estimates for the SCAR–B data set as determined by the GOES-8 ABBA (version 5.5) have changed substantially from the values reported during SCAR–B. The diffraction correction and variable offset for cloud contamination in version 5.5 result in fire size estimates that are, on average, 75% less than originally reported with version 1.0. Comparison with ground

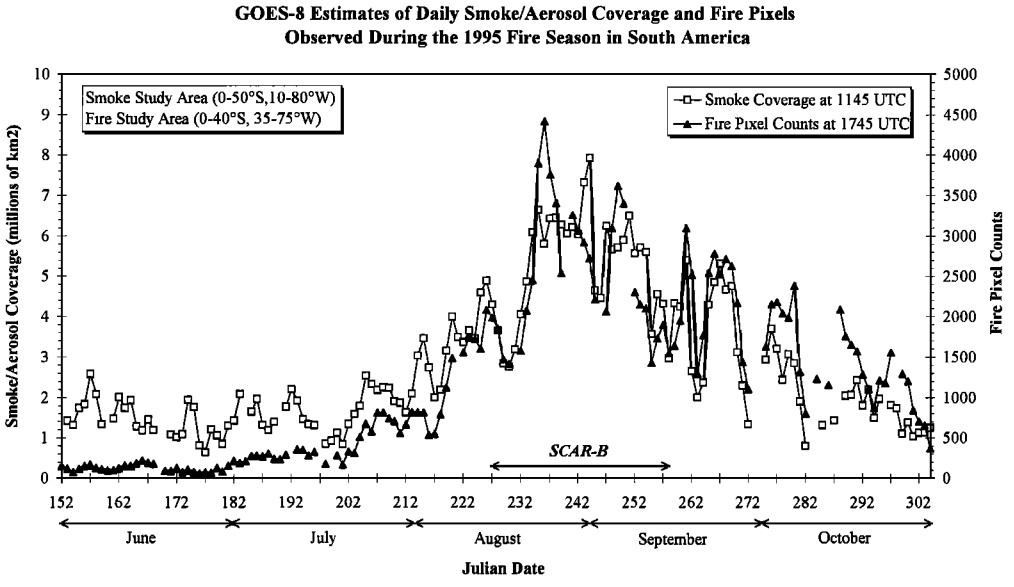

Figure 3. Time series depict daily GOES-8 ASADA estimates of smoke/aerosol coverage at 1145 UTC and GOES-8 ABBA fire pixel counts at 1745 UTC during the 1995 fire season. The largest smoke palls are seen in the months of August and September at the peak of the burning season. Day-to-day variability in smoke coverage tracks similar fluctuations in fire activity.

truth indicates that GOES ABBA (version 5.5) estimates are more representative of actual burning conditions.

6. GOES-8 ASADA Results for SCAR–B and 1995 Fire Season

Investigations have shown that although smoke in South America can be identified in GOES-8 visible observations throughout the day, the best observing time is in the morning near 1200 UTC. The GOES-8 satellite viewing angle, solar illumination, and regional meteorology combine to form the optimal observing conditions at this time [*Prins and Menzel*, 1992, 1996]. GOES-8 multispectral data collected daily at 1145 UTC during the 1995 fire season (June–October) were processed with the GOES-8 ASADA in an effort to catalogue the extent and relative intensity of smoke/aerosol coverage. The aerosol monitoring study area extended from 0° to 50°S and 10° to 80°W, including most of the continent of South America and the South Atlantic Ocean. A time series of GOES-8 ASADA estimates of daily smoke/aerosol coverage is presented in Figure 3. From June to mid-July the average areal extent of smoke/aerosols remained fairly constant at ~1.5 million km^2 and included smoke from biomass burning as well as other anthropogenic and naturally occurring aerosols. During the last two weeks in July the smoke/aerosol coverage began to increase dramatically to a maximum of 7.9 million km^2 on September 1, 1995. Smoke/aerosol coverage decreased to background levels in late October. During the months of August and September the average daily smoke pall size was of the order of 4.5 million km^2, 3 times greater than values recorded at the beginning of the season. The increased smoke/aerosol coverage observed from mid-July through mid-October closely mirrored increases in biomass burning during this time (see Figure 3). Peak burning observed during the last week in August produced a large smoke pall covering over 6 million km^2 from August 22 to September 1, 1995. Throughout the fire season the day-to-day variability in aerosol coverage reflected fluctuations in GOES-8 ABBA observed biomass burning activities. Even relatively small fluctuations in fire pixel counts had corresponding responses in smoke/aerosol coverage (e.g., September 14, 1995). A simple cross correlation between fire counts at 1745 UTC and smoke coverage at 1145 UTC was calculated at different lags. The results showed the highest cross correlation (correlation coefficient of 0.86) at lag zero. This indicates that the peak in GOES-8 detected smoke coverage at 1145 UTC precedes the peak in fires at 1745 UTC. It is possible that the regional extent of smoke coverage is at a maximum prior to the peak in detected fire pixels followed by a maximum in regional smoke loading. Further work will be done to analyze this.

Plate 5 presents an overview of the distribution and relative intensity of smoke (on a 0.5° grid) as determined by the GOES-8 ASADA at 1145 UTC throughout the Amazon basin and the South Atlantic for SCAR–B (Plates 5b, 5d) and the 1995 fire season (Plates 5a, 5c). Plates 5a and 5b show the percentage of time the GOES-8 ASADA reported smoke/aerosol for a given location from June to October and during SCAR–B, respectively. The seasonal composite shows the highest smoke/aerosol occurrences along the front range of the Andes Mountains in Bolivia and also in Rondonia, Brazil. During SCAR–B a large portion of South America east of the Andes was covered with smoke over 80% of the time. The regions most often affected by smoke are collocated with or downwind of the most intensive burning regions (see Plate 4). Similar observations have been reported for SCAR–B using NOAA AVHRR and UV radiance measurements from the Global Ozone Monitoring Experiment (GOME) instrument [S. Christopher, personal communication, 1997; *Gleason et al.*, this issue].

During the dry season, anticyclonic flow is predominant throughout the Amazon Basin. Easterly winds in the northern part of the Amazon Basin transport the aerosols westward toward the Andes Mountains. The aerosols accumulate along the front range of the Andes before being channeled to the south-southeast where they can be transported over the South

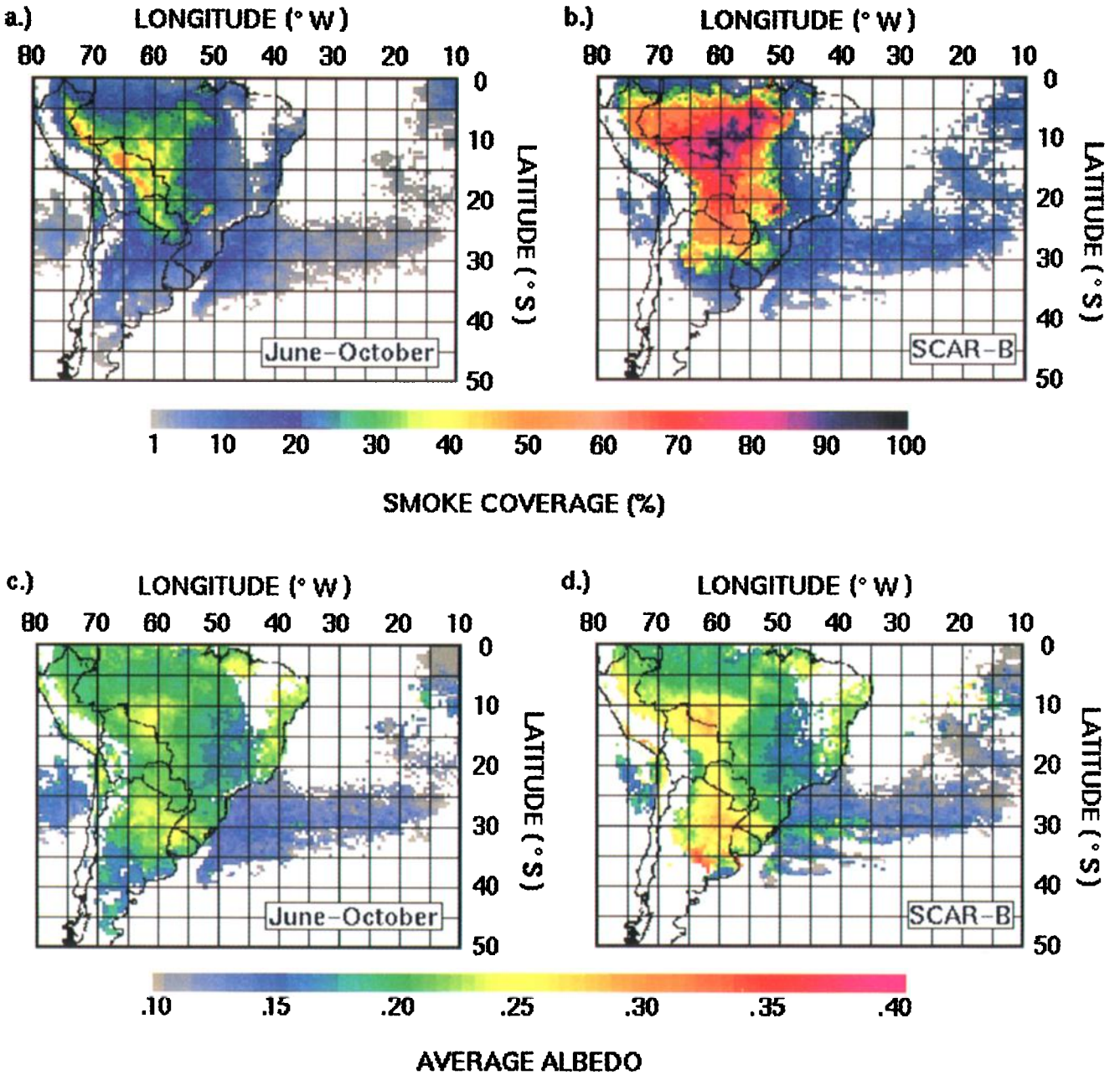

Plate 5. (a and b) Percentage of time a given area (on a 0.5° grid) was smoke covered at 1145 UTC from June to October 1995 and during SCAR–B, respectively. (c and d) Average GOES-8 ASADA derived smoke albedo for the same time periods. The smoke albedo is derived from the GOES-8 visible band (0.52–0.72 μm). The highest GOES-8 ASADA derived smoke albedos are collocated or downwind of regions with the greatest fire activity (see Plate 4).

Atlantic Ocean ahead of frontal boundaries which often form in this region [*Hsu et al.*, 1996; *Prins and Menzel*, 1996a, b; *Herman et al.*, 1997; *Stowe et al.*, 1997]. The GOES-8 ASADA results suggest that during SCAR–B, transport over the South Atlantic Ocean at 30°S occurred 30% of the time, with long-range transport occurring less frequently. Manual inspection of GOES-8 imagery indicated that transport over the South Atlantic occurred more frequently, but the signature was often very weak and difficult to discriminate from thin cirrus. Smoke transport patterns observed in GOES-8 visible imagery and in the ASADA product were compared with NCEP model output. Flow patterns in NCEP model output at 700 mbar were similar to that observed in the GOES-8 imagery and derived smoke product (see Plate 1b).

The GOES-8 ASADA derived albedo composites for SCAR–B and the 1995 fire season show the highest values in the states of Para, Mato Grosso, and Rondonia, Brazil, and in Bolivia, Paraguay, Northern Argentina and Uruguay, where derived smoke albedo estimates are 2 to 3 times higher than clear background values. During the last week of August and the first week of September the GOES-8 ASADA recorded derived albedos as high as .40 in central Brazil and Bolivia. Aircraft and ozone sounding measurements in the vicinity of Cuiabá and Alta Floresta reported elevated ozone readings

during this time [*Thompson et al.*, 1977; *Kirchhoff et al.*, 1997]. Surface observations in Cuiabá (16°S, 56°W) and Alta Floresta (10°S, 56°W) reported elevated aerosol mass concentrations associated with increased fire activity at the end of August [*Artaxo et al.*, this issue]. Higher concentrations were detected in Alta Floresta, with the fine particle mode and black carbon concentrations 4 times greater than in Cuiabá. GOES-8 ASADA results frequently show the smoke from fires in Mato Grosso, Brazil, impacting Alta Floresta, while Cuiabá is generally on the eastern edge of the smoke pall as seen on August 28, 1995 (see Plate 1b). Several days later as the smoke pall increased in size, the GOES-8 ASADA reported the smoke pall directly over Cuiabá. The increase in aerosol loading at Cuiabá was also documented by irradiance and aerosol optical thickness values calculated from surface measurements made at the Cuiabá site from August 27 to September 1, 1995 [*Holben et al.*, 1997; *Eck et al.*, this issue]. During this period, manual inspection of diurnal GOES-8 multispectral imagery seemed to indicate reduced afternoon cumulus cloud development in areas with high aerosol loading in the 1145 UTC imagery possibly due to reduced surface heating during the day. A more rigorous analysis will be done to quantitatively investigate these observations.

7. Conclusions

Over the past 2 years the GOES-8 ABBA and ASADA have matured based on input from the SCAR–C and SCAR–B field programs. Algorithm development activities have resulted in more robust algorithms for fire and smoke identification and characterization. The SCAR–B field program provided a unique opportunity to develop and test the GOES-8 ABBA and ASADA with in situ ground truth and remote sensing measurements for comparison and validation. The GOES-8 ABBA was able to identify fires of the order of a few acres in size. A comparison between the GOES-8 ABBA (version 5.5) fire size estimates and two SCAR–B prescribed burns showed that although the GOES-8 ABBA results only provide an instantaneous snapshot of fire activity, estimates are typically in line with ground truth observations (within 20–50% for small fires). This validation exercise also suggested the utility of considering a time series of half hourly GOES-8 ABBA estimates to better characterize diurnal burning.

GOES-8 data (1145, 1445, 1745, and 2045 UTC) collected during the 1995 fire season (June–October) were reprocessed with version 5.5 of the GOES-8 ABBA. Diurnal results demonstrate the need for geostationary fire monitoring in the tropics. Although peak burning usually occurs in the middle of the afternoon local time, fires are lit throughout the day with flaming conditions only lasting for a short time. Daily totals of unique fire pixels observed at all four time periods with the GOES-8 ABBA were typically 65% greater than the value at 1745 UTC. Only 20% of the fire pixels were detected in more than one time period. Nearly 340,000 fire pixels were detected with the GOES-8 ABBA from June to October 1995 with an estimated total burned area of ~42,000 km^2. Roughly 40% of the burning occurred during the SCAR–B field program with ~3500 unique fire pixels detected per day from August 15 to September 15. Most of the burning was concentrated along the perimeter of the Amazon. Many fires were also detected in Bolivia, Paraguay, and northern Argentina. A composite of fires for the entire season showed distinct burning patterns along rivers and in areas with recent road construction and associated settlements within Amazonia. On average, 35% (14,646 km^2) of the fire pixels were located in the broadleaf tropical forests; over 45% were located in the cerrado, shrub, and grasslands (18,830 km^2). These values are significantly less than reported with the GOES VAS ABBA in the 1980s [*Prins and Menzel*, 1994]. The GOES VAS ABBA product overestimated the amount of subpixel area burned for a given observation. The GOES-8 ABBA burned areas estimates are more realistic and represent what would be expected from snapshots of diurnal burning characteristics.

Multispectral GOES-8 data collected at 1145 UTC from June to October were processed with version 3.0 of the GOES-8 ASADA. The results show a sharp increase in smoke/aerosol coverage and intensity corresponding to peak burning in August and September and the first two weeks in October. During the months of June and July the average smoke/aerosol coverage extended over 1.5 million km^2. In August and September the average size of the smoke pall was of the order of 4.5 million km^2. At the peak of the burning season the GOES-8 ASADA detected a smoke pall extending over 7.9 million km^2 with derived smoke albedos 3 to 4 times higher than what was observed under clear conditions. The day-to-day variability in smoke coverage and intensity was directly linked to the amount of fire activity in the region.

Applications of the GOES-8 ABBA and ASADA during SCAR–B and the 1995 burning season demonstrate the improved capability of the GOES-8 instrument for monitoring diurnal, spatial and seasonal signatures in biomass burning in South America. GOES-8 fire and smoke products for SCAR–B and the 1995 season provide a benchmark in ongoing efforts to determine interannual trends in South American biomass burning from a geostationary platform from 1995 into the next century.

Acknowledgment. This work was sponsored by the National Aeronautics and Space Administration under contract NAGW-3804.

References

Andreae, M. O., Biomass burning: Its history, use, and distribution and its impact on environmental quality and global climate, in *Global Biomass Burning: Atmospheric, Climatic, and Biospheric Implications*, edited by J. S. Levine, pp. 3–21, MIT Press, Cambridge, Mass., 1991.

Andreae, M. O., et al., Biomass burning emissions and associated haze layers over Amazonia, *J. Geophys. Res.*, *93*, 1509–1527, 1988.

Artaxo, P., E. T. Fernandes, J. V. Martins, M. A. Yamasoe, P. V. Hobbs, W. Maenhaut, K. M. Longo, and A. Castanho, Large-scale aerosol source apportionment in Amazonia, *J. Geophys. Res.*, this issue.

Bywaters, K. W., and E. M. Prins, An interactive WWW tool for coupling satellite and meteorological data in real time, paper presented at the 12th International Conference on Interactive Information and Processing Systems (IIPS) for Meteorology, Oceanography, and Hydrology, *Am. Meteorol. Soc.*, Atlanta, Ga., 1996.

Christopher, S. A., D. V. Kliche, J. Chou, and R. Welch, First estimates of the radiative forcing of aerosols generated from biomass burning using satellite data, *J. Geophys. Res.*, *101*, 21,265–21,273, 1996.

Crutzen, P. J., and M. O. Andreae, Biomass burning in the tropics: Impact on atmospheric chemistry and biogeochemical cycles, *Science*, *250*, 1669–1678, 1990.

Crutzen, P. J., A. C. Delany, J. Greenburg, P. Haagensen, L. Heidt, R. Lueb, W. Pollock, W. Seilor, A. Wartburg, and P. Zimmerman, Tropospheric chemical composition measurements in Brazil during the dry season, *J. Atmos. Chem.*, *2*, 233–256, 1985.

Eck, T. F., B. N. Holben, I. Slutsker, and A. Setzer, Measurements of irradiance attenuation and estimation of aerosol single-scattering albedo for biomass burning aerosols in Amazonia, *J. Geophys. Res.*, this issue.

Fishman, J., P. Minnis, and H. G. Reichle Jr., Use of satellite data to

study tropospheric ozone in the tropics, *J. Geophys. Res.*, *91*, 14,451–14,465, 1986.

Fishman, J., V. C. Brackett, E. V. Browell, and W. B. Grant, Tropospheric ozone derived from TOMS/SBUV measurements during TRACE A, *J. Geophys. Res.*, *101*, 24,069–24,082, 1996.

Flasse, S. P., and P. Ceccato, A contextual algorithm for AVHRR fire detection, *Int. J. Remote Sens.*, *17*(2), 419–424, 1996.

Gleason, J. F., N. C. Hsu, and O. Torres, Biomass burning smoke measured using backscattered ultraviolet radiation: SCAR-B and Brazilian smoke interannual variability, *J. Geophys. Res.*, this issue.

Herman, J. R., P. K. Bhartia, O. Torres, C. Hsu, C. Seftor, and E. Celarier, Global distribution of UV-absorbing aerosols from Nimbus 7/TOMS data, *J. Geophys. Res.*, *102*, 16,911–16,922, 1997.

Holben, B. N., A. Setzer, T. F. Eck, A Pereira, and I. Slutsker, Effect of dry-season biomass burning on Amazon Basin aerosol concentrations and optical properties, 1992–1994, *J. Geophys. Res.*, *101*, 19,465–19,481, 1996.

Holben, B. N., D. Tanré, Y. Kaufman, I. Slutsker, and D. Ward, Single-scattering albedo approximated from ground based measurements of aerosol optical thickness in the Amazon Basin, in *SCAR-B Proceedings*, edited by V. W. J. H. Kirchhoff, pp. 73–78, Transtec Edit., São Paulo, Brazil, 1997.

Hsu, N. C., J. R. Herman, P. K. Bhartia, C. J. Seftor, O. Torres, A. M. Thompson, J. F. Gleason, T. F. Eck, and B. N. Holben, Detection of biomass burning smoke from TOMS measurements, *Geophys. Res. Lett.*, *23*(7), 745–748, 1996.

Justice, C. O., and P. R. Dowty, Technical Report of the IGBP-DIS Satellite Fire Detection Algorithm Workshop, February, 1993, NASA GSFC, Greenbelt, Md., *Tech. Rep. IGBP-DIS Work. Pap. 9*, Int. Geos.-Bios. Programme, Paris, 1994.

Kaufman, Y. J., and R. S. Fraser, The effect of smoke particles on clouds and climate forcing, *Science*, *277*, 1636–1639, 1997.

Kauffman, J. B., L. S. Guild, D. L. Cummings, E. A. Castro, L. Ellingston, R. Babbitt, and D. E. Ward, Total aboveground biomass, elemental pools, and combustion factors of fires sampled during the SCAR-B experiment, in *SCAR-B Proceedings*, edited by B. W. J. H. Kirchhoff, pp. 73–78, Transtec Edit., São Paulo, Brazil, 1997.

Kirchhoff, V. W. J. H., P. C. Alvala, and Y. Sahai, Ozone measurements from an aircraft platform during the SCAR-B field experiment, in *SCAR-B Proceedings*, edited by V. W. J. H. Kirchhoff, pp. 109–112, Transtec Edit., São Paulo, Brazil, 1997.

Levine, J. S., Biomass burning: Combustion emissions, satellite imagery, and biogenic emissions, in *Global Biomass Burning: Atmospheric, Climatic, and Biospheric Implications*, edited by J. S. Levine, pp. 264–271, MIT Press, Cambridge, Mass., 1991.

Matson, M., and J. Dozier, Identification of subresolution high temperature sources using a thermal IR sensor, *Photogramm. Eng. Remote Sens.*, *47*, 1311–1318, 1981.

Menzel, W. P., and E. M. Prins, Monitoring biomass burning and aerosol loading and transport utilizing multispectral GOES-8 data, paper presented at the 1996 International Symposium on Optical Science, Engineering, and Instrumentation, SPIE, Denver, Colo., 1996a.

Menzel, W. P., and E. M. Prins, Monitoring biomass burning with the new generation of geostationary satellites, in *Biomass Burning and Global Change*, edited by J. S. Levine, pp. 56–64, MIT Press, Cambridge, Mass., 1996b.

Olson, J. S., World Ecosystems (WE1.4). Digital Raster Data on a 10-minute geographic 1080 × 2160 grid, in Global Ecosystems Database, Version 1.0: Disk A. Boulder, CO: U.S. Dept. of Commer., Natl. Oceanic and Atmos. Admin., Natl. Geophys. Data Cent., Washington, D. C., 1992.

Penner, J. E., R. E. Dickinson, and C. A. O'Neill, Effects of aerosol from biomass burning on the global radiation budget, *Science*, *256*, 1432–1433, 1992.

Penner, J. E., R. J. Charlson, J. M. Hales, N. S. Laulainen, R. Leifer, T. Novakov, J. Ogren, L. F. Radke, S. E. Schwartz, and L. Travis, Quantifying and minimizing uncertainty of climate forcing by anthropogenic aerosols, *Bull. Am. Meteorol. Soc.*, *75*(3), 375–400, 1994.

Prins, E. M., and W. P. Menzel, Geostationary satellite detection of biomass burning in South America, *Int. J. Remote Sens.*, *13*, 2783–2799, 1992.

Prins, E. M., and W. P. Menzel, Trends in South American biomass burning detected with the GOES VAS from 1983 to 1991, *J. Geophys. Res.*, *99*, 16,719–16,735, 1994.

Prins, E. M., and W. P. Menzel, Monitoring biomass burning and aerosol loading and transport from a geostationary satellite perspective, paper presented at the Seventh Symposium on Global Change Studies, *Am. Meteorol. Soc.*, Atlanta, Ga., 1996a.

Prins, E. M., and W. P. Menzel, Investigation of biomass burning and aerosol loading and transport utilizing geostationary satellite data, in *Biomass Burning and Global Change*, edited by J. S. Levine, pp. 65–72, MIT Press, Cambridge, Mass., 1996b.

Skole, D., and C. Tucker, Tropical deforestation and habitat fragmentation in the Amazon: Satellite data from 1978 to 1988, *Science*, *260*, 1905–1910, 1993.

Stowe, L., A. M. Ignatov, and R. R. Singh, Development, validation, and potential enhancements to the second-generation operational aerosol product at the National Environmental Satellite, Data, and Information Service of the National Oceanic and Atmospheric Administration, *J. Geophys. Res.*, *102*, 16,923–16,934, 1997.

Thompson, A. M., D. P. McNamara, V. W. J. H. Kirchhoff, and A. Setzer, Tropospheric ozone at Cuiabá during SCAR-B and TRACE-A, in *SCAR-B Proceedings*, edited by V. W. J. H. Kirchhoff, pp. 191–194, Transtec Edit., São Paulo, Brazil, 1997.

Twomey, S. A., M. Piepgrass, and T. L. Wolfe, An assessment of the impact of pollution on the global albedo, *Tellus, Ser. B*, *36*, 356–366, 1984.

J. M. Feltz, CIMSS, University of Wisconsin-Madison, Madison, WI 53706.

W. P. Menzel and E. M. Prins, NOAA/NESDIS/ORA/ASPT, 1225 West Dayton St., University of Wisconsin-Madison, Madison, WI 53706. (e-mail: elaine.prins@ssec.wisc.edu)

D. E. Ward, Intermountain Research Station, U.S. Forest Service, Missoula, MT 59807.

(Received November 8, 1997; revised May 6, 1998;
accepted May 8, 1998.)